Geotechnical Safety and Risk V
T. Schweckendiek et al. (Eds.)

doi:10.3233/978-1-61499-580-7-61

Quantitative Geotechnical Risk Management for Tunneling Projects in China

Hongwei HUANG and Dongming ZHANG
Department of Geotechnical Engineering, Tongji University, China

Abstract. To date, the tunneling in China is experiencing an age of fast development for decades. The potential risks behind the huge amount of construction and operation works in China was first formally realized and managed after 2002. The transition of risk assessment from a qualitative manner to a quantitative manner is on the way from the research gradually to the practice. This paper tries to share some experiences in the quantitative risk management for tunneling in China by introducing novel techniques and associated practical applications. The fuzzy fault tree analysis is used for hazard identification, the conditional Markov chain for probability analysis of soil spatial uncertainty, the quantitative vulnerability analysis for consequence evaluation and the field data based statistics for environmental impact risk analysis. All these novel methods have been validated successfully by applying into real cases shown in the paper. The dynamic feature of risk management is appreciated due to the different stages and scenarios of a tunnel project. The real-time monitoring technique developed using the LEDs and MEMS coupled with WSN could visualize the risk to the worker on site timely. The resilience analysis model to incorporate the high-impact low-chance risk for tunnel lining structure is introduced in the end of paper, which could assist the engineers to make the decision on performance recovery strategies once the tunnel goes through a significant disruption.

Keywords. Risk Management, Tunnel Project, Vulnerability, Resilience, Risk Visualization

1. Introduction

It should be recognized that the development of geotechnical engineering in China these days is unbelievably fast. Hundreds of underground works have been constructed. However, there are huge amounts of risks behind these constructions since no projects could be risk free. It is reported that a deadly accident will happen every ten minutes in the civil engineering construction (ILO, 2003). The safety in operating the metro tunnel with a 538km mileage in Shanghai, for example, is worst concerned by the Shanghai municipal government. Risk in the constructions can be managed, minimized, shared, transferred or accepted. It cannot be ignored (Latham, 1994). A rational and integrated risk management is thus of great importance and help to support the decision making.

Risk, from the definition, is a combination of the frequency of occurrence of a defined hazard and the consequences of the occurrence (ITA, 2002). Casagrande (1965) has classified the risk into two major types. One is the engineering related, and the other is human related. In the engineering discipline, the former type is mostly emphasized, which is sub-divided into unknown risk and calculated risk. Hundreds of papers on the probability of hazard occurrence were published in the passed decades, selected masterpieces could be found in Ang and Tang (1975), Whitman (1984, 2000) and Lacasse (2015), but the lacking of quantitative evaluation of the hazard cost limits the risk assessment in a qualitative way, rather than in a quantitative way. Even for a risk that can be expressed by a numeric number, it is also a mystery for workers on site to understand clearly. Hence, the risk should be translated by a visualized manner (Huang, et al., 2013).

So far, the geotechnical risk has been introduced into the engineering practice in Chine for almost 10 years (Huang, 2006). In view of the above background, the 10 years experiences in practicing risk management for geotechnical engineering in China are shared by the authors in this paper. This paper will cover the management with respect to the time dimension, the quantitative method, design, code and project application. Finally, some

developments of the current research on risk visualization and resilience analysis for high-impact low-chance risk are emphasized. It should be pointed out at the first of the paper that the present work is applied and also limited by the experiences of the authors from mainland of China.

2. Lifetime Risk Management (LRM)

In China, the risk management for critical geotechnical infrastructures is not compulsory until recently. The milestone is the issue of the China national code for risk management of underground works in urban rail transit (GB50652-2011, 2012) (the Code in short hereafter). Before the Code, the risk management is carried out largely based on single stage that is not systematical and integrated. The safety of the infrastructure contains large uncertainty since potential high risk might be ignored due to the independent management at different project stages.

After the Code was put into effect in 2012, the lifetime management of risk for the critical infrastructures, such as metros in urban area, is carried out compulsorily. It covers the multiple stages, including planning stage, engineering feasibility stage, detailed design stage, construction stage and operation stage. The detail of the assessment for a specific stage is described in Figure 1 as a schematic. It should be noted that the earlier the risk is identified, the easier the risk can be managed.

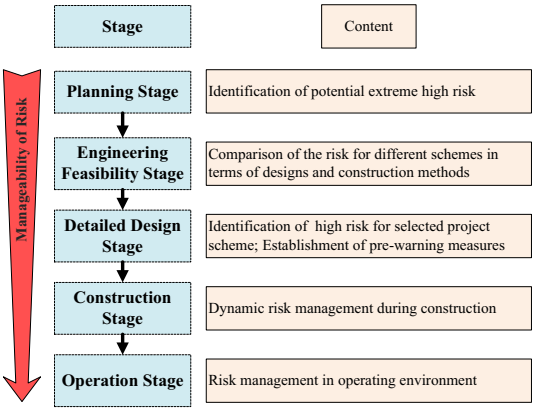

Figure 1. Schematic of lifetime risk assessment

3. Quantitative Risk Assessment (QRA)

Quantitative risk assessment (QRA) is a method of quantifying the degree of risk through a systematic examination of the hazard that threatens the tunnel safety. Quite often, it is evaluated by the multiplication of the probability of the occurrence of the hazard and the subsequent consequences if the hazard occurs, and is expressed as follows,

$$R = P(A) \cdot C(A) \tag{1}$$

Generally, four steps, i.e., hazard identification, probability analysis, consequence analysis and risk calculation, are necessary for an integrated quantitative risk assessment (QRA). Figure 2 plots a flowchart of the QRA (Liu, et al., 2009). To be more specific, the consequence could be sub-divided into the degree of system performance loss, i.e., vulnerability V and its corresponding cost E (Li, et al., 2010). Eq. 1 can be expressed in detail as below:

$$R(A) = P(A) \times V(A) \times E \tag{2}$$

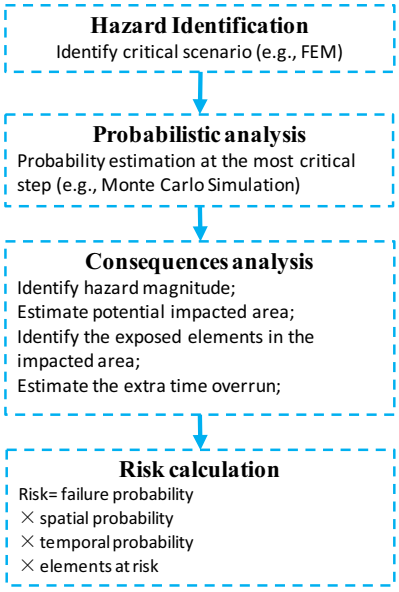

Figure 2. Flowchart of the QRA incorporating QCA

Following this sequence, the paper describes some methods or frameworks frequently used in the QRA for tunneling projects in China. Due to the page limit, only

the key principle of the method and its application into the tunnel case are presented briefly below.

3.1. Fuzzy Fault Tree Analysis (FTA) –Hazard Identification

It has been widely recognized that the damage of the tunnel is not likely to be caused only by a single hazard. There might be a chain effect between hazards. The fault tree (FT) is always built to systematically understand the growth path of a catastrophic event. A typical fault tree for the damage of the cutter of the earth pressure balance (EPB) shield machine in tunneling is shown in Figure 3 (Yan, et al., 2009). The top event can be triggered by a combination of the sub-event serially or parallelly. In this case, the cutter damage can be triggered by three major sub-events, i.e., poor ground condition, irrational construction and shield factor. In addition, the shield factor could be further triggered by three "sub-sub-events". Note that the cutter damage at the top of the tree also can be a sub-event for a more serious event, such as cutter failure or failure of the EPB machine.

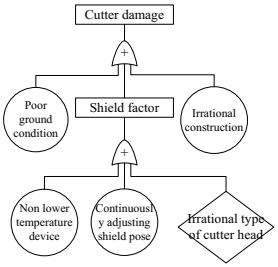

Figure 3. An example of fault tree analysis (FTA) for the cutter damage of EPB shield machine

When the events that cannot be further divided, i.e., basic events, are available, the probability of the occurrence of the top event can be calculated from Eq. 3 below,

$$P_T = 1 - \prod_{i=1}^{n} [1 - P(M_i)] \tag{3}$$

$P(M_i)$ is the probability of the occurrence of a minimal cut sets of the events that could directly trigger the occurrence of the top event. The independency between minimal cut sets is assumed in the calculation. However, the probability for the basic event is usually difficult to be quantified. Hence, the fuzzy set theory is adopted to cope with it. A triangular possibility distribution of the probability of the occurrence of the basic event is used and plotted in Figure 4 (Bian and Huang, 2006). Then the fuzzy probability of the top event can be expressed as triangular fuzzy numbers and the parameters. It reflects the robustness of the calculated probability of the top event.

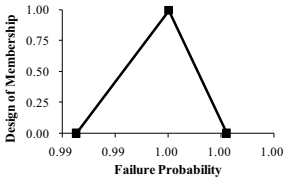

Figure 4. Possibility distribution of basic event probability

The main basic events affecting the occurrence probability of the top event can be determined and some effective measures are verified by sensitivity analysis to reduce occurrence probability of the basic events and the top event. The sensitivity of basic event can be evaluated by the index V_i as below:

$$V_i = \frac{\partial g(x)}{\partial x_i}\bigg|_{x=\mu_{xi}} \frac{\mu_{xi}}{\mu_g} \tag{4}$$

where μ_g is the occurrence probability of the top event, μ_{xi} is the average occurrence probability of the basic event x_i.

3.2. Conditional Markov Process (CMP) for Soil Distribution Probability

The uncertainty in the tunneling can be largely attributed to the uncertainty of the spatially varied soils along the tunnel longitudinal direction. The limited site investigation in terms of the borehole numbers is the major source that creates the soil uncertainties. It is customary to linearly characterize soil layering between boreholes. However, the tunnel failures are usually caused by the underestimation of the complex distribution of the layered soils. In view of this limitation, the conditional Markov process (CMP) can be adopted to fully utilize the existing borehole

data in the prediction of the soil distribution between two adjacent boreholes incorporating the uncertainties.

The schematic of the CMP is plotted in Figure 5 (Hu and Huang, 2007). The field can be meshed into the separate elements as shown in Figure 5. The soils in a borehole can be divided into N_j elements vertically and N_i element horizontally. The n types of soil, so called n status, randomly locates in these elements. Each element represents only one of those n status. The CMP is thus adopted to characterize the probability of a specific type of soil for an interested element. The characterization can be expressed mathematically by Eq. 5 below

$$p_{l,m\to k|q} = C' \cdot p^x_{lk|q} \cdot p^z_{mk} = \frac{p^x_{lk} \cdot p^{x(N_x-i)}_{kq}}{\sum_f p^x_{lf} \cdot p^{x(N_x-i)}_{fq} \cdot p^z_{mf}} p^z_{mk} \quad (5)$$

$$f = 1,2,\cdots,n; k = 1,2,\cdots,n$$

where C' is a normalized coefficient, the $p^x_{lk|q}$ is the conditional probability of the soil type k for the element (i,j) given the type l for the element $(i\text{-}1,j)$ and the soil type q for the borehole element (N_i,j) in the same row. The p^z_{mk} is the conditional probability of the soil type k for the element (i,j) given the type m for the element $(i,j\text{-}1)$.

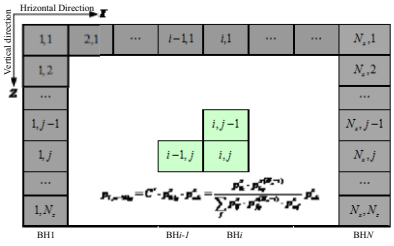

Figure 5. 2D model of conditional Markov process (CMP)

It is clear that the key parameters of CMP are the soil transition matrix which reflects the probability of soil transforming from one type to the other. It is established through dividing the soil sequence of borehole into different soil elements. Then the frequency of one type of soil transforming to the other in the next borehole element is calculated as the transition probability. As the borehole number increases, the sample size for the transition matrix grows. The accuracy of the soil distribution between two boreholes will thus increase as well. More importantly, the probability of soil distribution could reflect the possibility of the sandy or gravel lens in the silty soft clays in a more rational way.

The above described CMP model has been applied into the quantitative risk assessment for Yangtze river tunnel with respect to the longitudinal soil distribution along the alignment. Figure 6 has plotted the simulations of the soil profile by using the CMP model. When only three boreholes are available, the Monte Carlo simulation is carried out to produce a typical, i.e., most likely, soil profile. When the borehole number increases to five, the soil profile is updated. With the help of this model, the optimum borehole number is obtained when the update of the soil profile is not significant as the number increases.

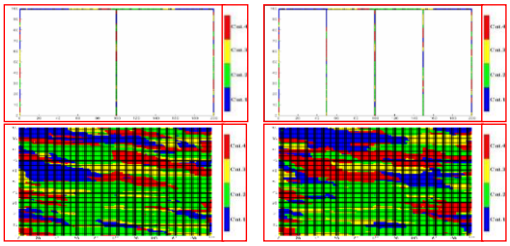

Figure 6. Simulation of soil layers probabilistic distribution by the 2D CMP under different boreholes data

3.3. Vulnerability Analysis

It is widely accepted that the vulnerability could be used to define the degree of the performance loss of the geotechnical structure subjected to a typical hazard. Vulnerability (V) here is defined as a function of the hazard intensity (I) associated with exposed elements at risk and the resistance ability (R) of the elements to withstand a threat (Uzielli, et al., 2008). It can be mathematically expressed by Eq. 6 (Li, et al., 2010). The system vulnerability varies with the intensity and resistance non-linearly, as described in Figure 7. The characterization of hazard intensity I and the system resistance R could be different from case to case.

$$V = f(I,R) = \begin{cases} 2\dfrac{I^2}{R^2} & \dfrac{I}{R} \le 0.5 \\ 1.0 - \dfrac{2(R-I)^2}{R^2} & 0.5 < \dfrac{I}{R} \le 1.0 \\ 1.0 & \dfrac{I}{R} > 1.0 \end{cases} \quad (6)$$

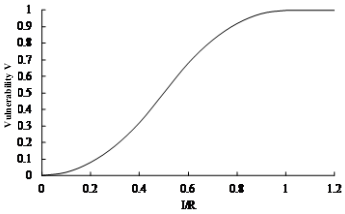

Figure 7. General vulnerability curve expressed by Eq. 6

This quantitative evaluation of the system vulnerability has been applied successfully into the case of the convergence performance of the existing shield tunnels induced by the above deep excavation (Huang and Huang, 2013). A typical example of the characterizations of the hazard intensity I, e.g., excavation depth H_c, and the tunnel resistance R, e.g., soil stiffness, is presented in Figure 8. Then the vulnerability V of the tunnel convergence performance can be calculated by using the above Eq. 6 corresponding to a specific intensity level and resistance level.

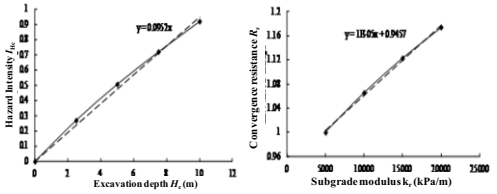

(a) Intensity (b) Resistance

Figure 8. Vulnerability of the convergence subjected to the deep excavation above the tunnel

By applying the analysis similar to that for the case described above, the vulnerability of the performance of segmental lining subjected to the extreme surcharge hazard is plotted in Figure 9 (Shen, et al., 2014).

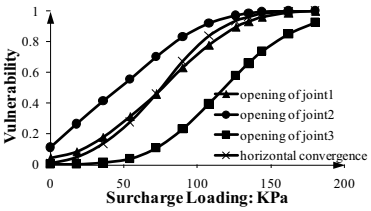

Figure 9. Vulnerability curves for tunnels subjected to the surcharge

3.4. Quantitative Consequence Analysis (QCA)

It should be realized that the consequence depends on the exposure place and the exposure time to the risk event. Besides the vulnerability and the cost of the loss, the time and space dependency should be included in a detailed quantitative consequence analysis. Eq. 2 is thus revised by a refined equation below,

$$R_E(A) = P(A) \times P(T|A) \times \sum \left(P(S|A) \times V(A|S) \times E \right) \quad (7a)$$

$$R_H(A) = P(A) \times P(T|A) \times \sum \left(P(S|A) \times V(A|S) \right) \quad (7b)$$

where Eq. 7a is referred to the economic loss and Eq. 7b is referred to the human loss. $P(T|A)$ is the conditional probability of the hazard happened in the time interval T, and $P(S|A)$ is the conditional probability of the hazard happened in the space area S. E stands for the value of the economic loss.

The above complex analysis of the consequence in terms of the summarization of all the conditions can be visually explained by the event tree, as shown in Figure 10 (Li, et al., 2014). The expectation of the consequence of the events in last column of the tree is essentially expressed by Eq. 7 mentioned above.

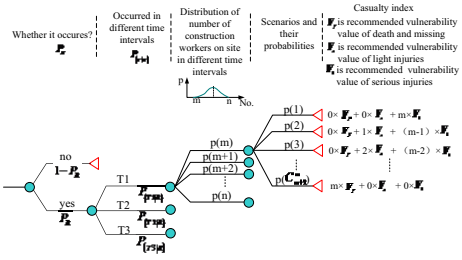

Figure 10. An example of event tree analysis (ETA) in QRA for shallow tunnels

The quantitative consequence analysis has been applied into the real case of the risk assessment for a mountain tunnel in Yunnan, south of China. Figure 11a described the layout of the mountain tunnel excavated by NATM method following the sequence denoted in the figure. Then the Monte Carlo simulation is adopted given the distribution of the corresponding type of loss, including the casualty, economic and the time overrun. By using the event tree analysis together with Eq. 7, the quantitative risk of the tunnel excavated by using this scheme can be calculated. Hence, it should be helpful to the decision-makers in that the quantitative risk assessment is more rational and comparable.

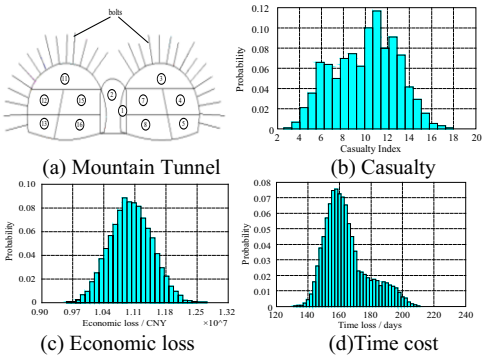

(a) Mountain Tunnel (b) Casualty

(c) Economic loss (d)Time cost

Figure 11. Probability density function of different type of consequence for mountain tunnel (Li, et al., 2014)

3.5. Risk Analysis of Tunneling Impact on Closed Structures

The ground movement induced by tunneling is always considered as the most risky event for a tunnel project in congested urban area, such as in Shanghai. The ground loss in tunneling will cause non-uniform ground settlement, which further deteriorates the structural performance of the buildings above ground surface, of the pipelines, existed tunnels and deep foundations in the subsurface. Among these impacts, the performance of buildings with shallow foundations might be the most vulnerable for its differential settlement, cracks or even collapse. Burland and Wroth (1975) has set up a general qualitative criteria for the on-ground structure damage level caused by underground constructions. Five levels, i.e., “undamaged”, “aesthetic damage”, “functional damage”, “structural damage” and “collapse”, are proposed in a sort of serious degree. Practically, this criteria should be transformed into a engineering-based language that is better for communication with worker on site.

Huang and Chen (2006) has established a quantitative damage loss curve to include the above damage levels by collecting more than one hundred of the field case of the building damages, shown in Figure 12.

$$C_H = \lambda m = \lambda m'\left(1 - nq_1q_3\right)q_2 \tag{8}$$

Where λ is the loss ratio of building. C_H is the direct loss of building damage. m is the practical value of the building before damage. m' is the original cost of building. q_1 is the percentage of wear and tear (when the service life is 50 years, it equals 2%). q_2 is the factor considering the inflation of prices. q_3 is the factor considering special maintenance (for minor repair and medium repair, it equals 1, and for others it is 0.7). n is the years in use. Different types of structural failures are considered in this model, including the concrete cracks and the building gradient. The horizontal axes stand for the ratio of moment to settlement indicating the ground movement. The vertical axes stand for the direct structural damage in terms of the property losses. It should be noted that for a same ground movement, the damage level of a building could be different from each other due to difference of foundation types, structure operated life time and etc. The effect of the structural factor mentioned above has been considered in this field-data-based model using a factor β, denoted as ratio of length to height of building. The criteria for β of masonry structure, no-piled frame structure, no-piled masonry structure and other structures are all included in the proposed model.

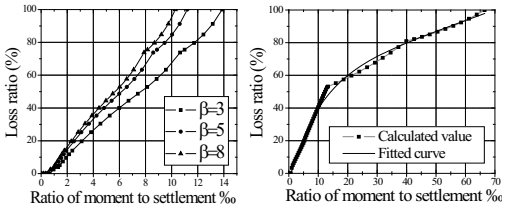

(a) concrete crack (b) gradient

Figure 12. Different damage ratio against the ground settlement: (a) concrete crack damage and (b) building gradient damage

3.6. Multi-source Risk Analysis by Bayesian Network

The Bayesian method is a natural tool for processing geotechnical information, highlighted by Professor Tang W. H., the pioneer on the reliability of geotechnical engineering (Tang, 1984; Zhang, et al., 2009). Bayesian updating can be assimilated to "the past as a guidebook for the future". The Bayesian network (BN) is the graphical representation of knowledge for reasoning under uncertainty. Because of its ability to combine domain knowledge with data, encode dependencies among variables, and learn causal relationships, it is a useful tool for quantitative risk assessment in geotechnical engineering. The BN is a probabilistic model based on directed acyclic graph:

$$B_s = G(Z, E) \tag{9}$$

where B_s represents the structure of the network, Z is the set of random variables (Z_1, Z_2, … Z_n), and $E \subseteq Z \times Z$ is the set of directed arcs, representing the probabilistically conditional dependency relationships among random variables.

One important property of the BN is that the joint probability function of all random variables in the network can be factorized into conditional and unconditional probabilities implied in the network (Nadim and Liu, 2013). Thus, the joint distribution can be expressed in the compact form as

$$P(z_1, z_2, ..., z_n) = \prod_{i=1}^{n} P\left(z_i \middle| pa(Z_i)\right) \tag{10}$$

where $pa(Z_i)$ is the parent set of z_i. It should be noted that if child node z_i has no parents, then the equation reduces to the unconditional probability of $p(z_i)$.

A simple Bayesian network structure for the structural performance of the tunnel lining under the disruption caused by the extreme surcharge above the tunnel is plotted in Figure 13.

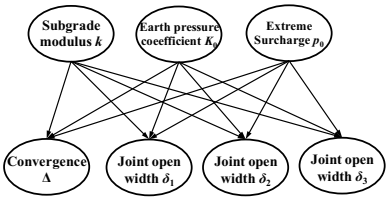

Figure 13. A typical BN structure for the structural performance of the lining subjected to the surcharge

When the evidence is available as the input for the net, the updating of the related conditional probabilities can be done straightforward by using the commercial software Netica. An example of the updated results of the above BN structure is illustrated in Figure 14.

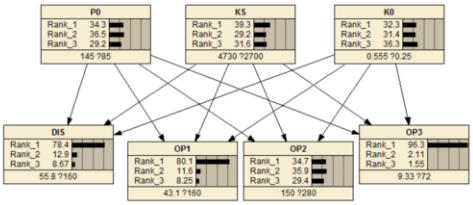

Figure 14. Bayesian networks analysis for shield tunnel deformation

4. Dynamic Risk Assessments (DRA)

As mentioned in Eq. 7, risk is regarded to be closely related to the time when the hazard happens. Hence, it should be a dynamic process for a detailed risk assessment in geotechnical engineering. This section will describe some implementation of the dynamic risk assessment (DRA) for the tunneling projects.

4.1. Data-Based DRA

Monitoring data directly indicate the safety and health of structures for risk early-warning strategies. The monitoring data based DRA consists of three major parts, including project monitoring, design of the risk warning index and subsequent dynamic risk assessment. The risk warning index is determined by the design requirement for the interested performance and the risk correction factor. The former one is calculated through the mechanical analysis under the dynamic construction conditions and the latter one is obtained by analyzing the corresponding performance of the structure apart from mechanical perspective. The flowchart for monitoring data based DRA is shown as Figure 15.

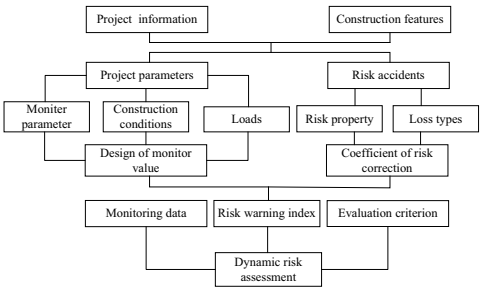

Figure 15. Flowchart of the monitoring data based DRA

4.2. Accidents-Based DRA

It should be noted that there are many other kinds of non-structural risks which cannot be assessed based on the monitoring data. Alternatively, these risks can be analyzed based on the recorded accidents adopting the methods such as Fault Tree Analysis (FTA), Analytic Hierarchy Process (AHP) or both.

For instance, a typical method combining the FTA and AHP for dynamic risk assessment is described here. First, the project is divided into several hierarchies, where the element of the lowest hierarchy is used as the top event of a fault tree, and corresponding risk accidents are registered. Then, FTA method is used to calculate the occurrence probability of the top event. Finally, AHP method is used to get the risk loss weight of each element and the dynamic risk based on recorded accidents is evaluated. The flowchart of the present recorded accidents based DRA is shown in Figure 16.

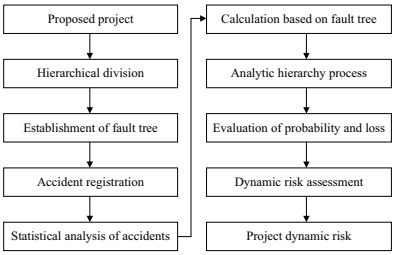

Figure 16. Flowchart of recorded accidents based DRA

A detailed FTA based dynamic risk assessment is illustrated in Figure 17. Essentially, the calculation process is similar to the traditional FTA described previously. However, note that the basic event as the fundamental event in a fault tree is extracted from the registered accidents from the records previously. Those accidents might not be closely related to the structural response of a geotechnical system.

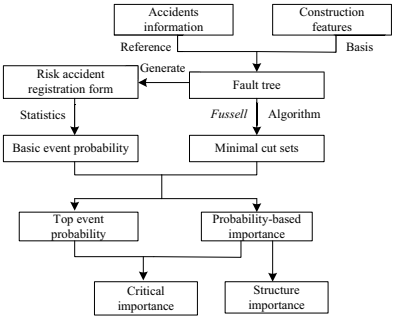

Figure 17. Application of FTA in accident based DRA

4.3. Scenario-Based DRA

For some of the geotechnical constructions such as deep excavations or the tunneling by NATM method, the sequence of different scenarios is quite crucial in determining the risk level for separate construction steps. Hence, the scenario-based, or the sequence-dependent, dynamic risk assessment is of great importance to manage the integrated risk during the construction.

The scenario-based DRA is defined as the product of scenario-based failure probability $P_f(t)$ and the scenario-based consequence $C(t)$. The t stands for the time for different scenarios.

The failure consequence consists of initial investment $C_I(t)$ and the additional loss such as casualties, construction delay and impact on neighboring buildings. For computational convenience, a coefficient ξ is introduced to quantify the relationship between the total consequence $C(t)$ to the initial investment $C_I(t)$. The scenario-based risk of the geotechnical structure can be expressed as follows,

$$R(t) = P_f(t) \times C(t) = \xi P_f(t) C_I(t) \qquad (11)$$

Figure 18 shows a deep excavation project in Shanghai. The scenario-based DRA is conducted with the help of a FEM model using Monte Carlo simulation.

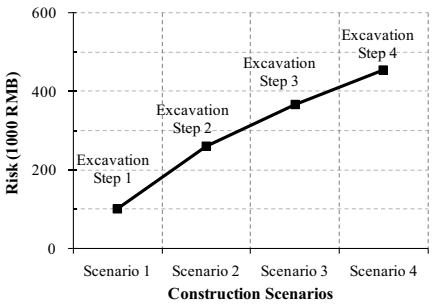

Figure 18. Scenario-based risk against construction steps

5. Standardization for Risk Management and Risk-Based Tunnel Design

5.1. Standards on Risk Management in China

In China, the standardization for risk management and assessment was commenced in HongKong in 2005 (CEDD-GEO, 2005), i.e., "Guidelines for Risk Management of Geotechnical Engineering in Hongkong". So far, a national code for urban rail transit system (GB50652-2011, 2012) and two national guidelines, i.e., one for railway tunnel (MRPRC, 2007) and the other for underground structures (MOHURD, 2007), have been put into effect regarding to the risk management. As for the risk assessment, there are two national guidelines for road tunnel (MTPRC, 2010, 2011) and a regional code for the urban rail transit system (DB11/1067, 2013).

5.2. Risk-based Tunnel Design

Considering the uncertainty in geotechnical engineering, the concept of risk management has been introduced into the design of the tunnel linings. The risk based tunnel design is carried out by applying the routine design method combined with the quantitative risk assessment. Three major parts are included in this design process, which are the assessment of the geological condition, the assessment of the risk for alternative design schemes and the decision-making for the most risk-friendly scheme of the tunnel design. A detailed flowchart of the procedure for the risk based tunnel design is illustrated in Figure 19.

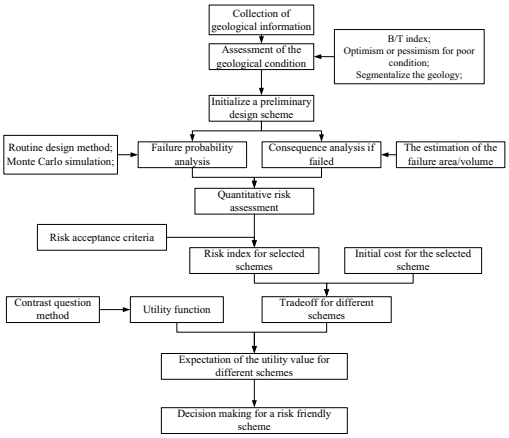

Figure 19. Flowchart of the procedure for the risk based tunnel design

The expectation of the tradeoff in Figure 19 for a selected design scheme can be calculated by the following equation,

$$E(A_i) = \sum_{j=1}^{k} R_{ij} \cdot P(S_j) \qquad (12)$$

where $E(A_i)$ is the expected tradeoff of selected i^{th} design scheme, $P(S_j)$ is the probability of the designed tunnel at the j^{th} status and the R_{ij} is the corresponding tradeoff value for the designed tunnel at the j^{th} status.

5.3. Development of Risk Software and Platform

The above mentioned quantitative risk assessment has been compiled into commercial softwares written based on the program of MATLAB and C++. Figure 20a is an integrated risk assessment and risk management software with a large database of the recorded accidents in tunneling around the world. Figures 20b and 20c show two project-based safety and risk monitoring and inquiry systems. Figure 20d is a web-based risk management platform for the construction of tunnels, which can be monitored and operated online far away from the construction site.

6. Visualization of Risk Assessment (VRA)

The traditional procedure of the risk pre-warning is that 1) firstly, the monitoring data are collected manually on site; 2) then the collected data is back analyzed indoors and the risk is assessed based on these data; and 3) finally, the risk pre-warning is sent out if the result of analysis is beyond the design criteria.

(a) TRM 2.0 (b) SRM

(c) SRR (d) RMP

Figure 20. Platform and software for risk management

Quite often, the time cost for this procedure is so significant that usually loses the merit of the "pre-" warning. The undefined measurement frequency could lead to the lack of adequate detection of anomalies and trends, accidents, higher costs for tunnels (ITA, 2014). In view of this circumstance, a real-time risk pre-warning system for geotechnical construction should be necessary to retain the feature of the response speed. In other words, the real time pre-warning system could make the risk visualized. Here, two types of the visualization techniques adopted in China nowadays will be briefly introduced below.

6.1. LEDs Aided Risk Visualization

The first visualization technique is developed based on the Light Emitting Diode (LEDs). The signal to capture the structural performance, the risk assessment based on the captured performances and the risk transformation from the assessed level of the risk to the visualized optical signal are all compiled in a microprocessor using the internal program. Finally the risk level of the construction could be reflected directly by the change of the colors of the LEDs on site. The whole process of risk visualization is controlled automatically by the computer, that enables the risk pre-warning system to be rational, real-time and visible.

Different kinds of sensors could be integrated in this LEDs aided visualization system. The specific choice of the sensors depends on the type of structural performance that the engineers are interested in. It is until the threshold for each level of risk has been set that the system is activated to work. Once the measured data exceed the pre-set threshold, the system will then change the corresponding LEDs color and flash the LEDs to make a on-site warning automatically.

For some important tunneling projects, the wireless transmission technology is used to connect the microprocessors and the remote output terminal. In this way, the remote risk pre-warning is achieved besides the on-site risk pre-warning. And also the memory chips can store the real time measured data for later check and analysis. The whole module of this system is illustrated in Figure 21.

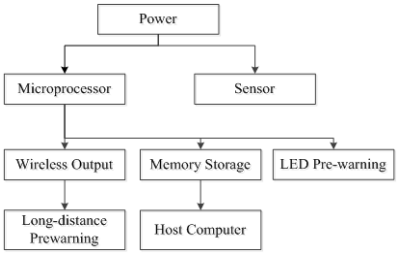

Figure 21. Schematic of LEDs aided risk visualization system

Figure 22 shows an application of the system into deep excavation in Shanghai. It proves that the monitoring and risk pre-warning by this LEDs aided risk visualization system is reasonable and feasible. The system should be helpful to the risk control in tunneling as well.

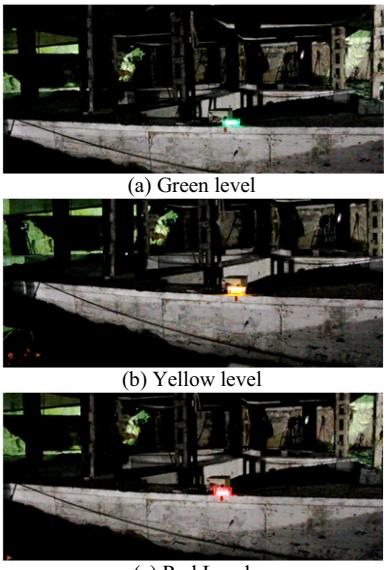

(a) Green level

(b) Yellow level

(c) Red Level

Figure 22. Application of risk visualization system into a deep excavation in Shanghai

6.2. WSN and MEMS Aided Risk Visualization

Recently, the micro electro-mechanical system (MEMS) and wireless sensor network system (WSN) are integrated and introduced into the smart geotechnical structure health monitoring systems. By using the indoor experiments of the MEMS and WSN system, the applicability and the accuracy of this smart risk visualization system has been validated (the experiment apparatus can be seen in Figure 23).

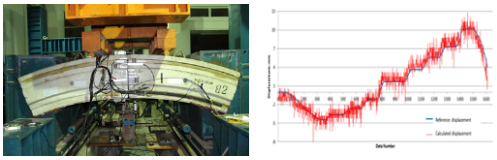

(a) experiments (b) results comparison of MEMS

Figure 23. Indoor test for the applicability

The developed MEMS and WSN system has been successfully applied into a metro tunnel in Shanghai, as shown in Figure 24. It has been proved by the real tunnel application that the MEMS and WSN smart system has great benefits for real-time structural monitoring.

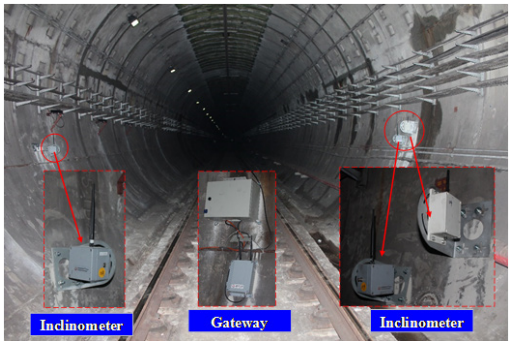

Figure 24. Application of the MEMS and WSN system into Shanghai metro tunnel

7. Tunnel Lining Resilience

As the key component of urban underground engineering and lifeline projects, the risk associated with the tunnel safety has become the focus of the government and the public in China. However, the current research and practice regarding engineering risk is subjected to a key deficiency in that while a lot of efforts have been exerted on risk assessment, little has been done for risk control both before and after the risky event, let alone the tunnel recovery after a real disaster. The fundamental and application-oriented research on the risk control and system resilience subjected to unfavorable environment are thus of great importance to better understand the risk,

especially for those high-impact low-chance risk.

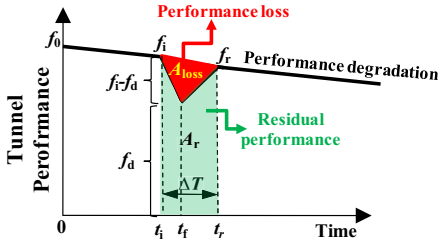

Figure 25. Disruption of tunnel performance subjected to extreme activities

It is widely realized that the resilience concept is gaining more and more attentions for the research on disaster relief. To the authors' knowledge, the resilience can be straightforwardly extended from performance degradation caused by the material aging effect. Figure 25 has illustrated the basic concept of resilience and the associated degradation curve. If there were no deadly threats acting on the tunnels, the performance should be degraded from initial f_0 to a certain f_i caused by the material aging effect (represented by a linear one in Figure 25). However, once the threat acts on the tunnels at time t_i, the performance will experience a dramatic decrease until a residual f_d has been reached to. By applying repair or rehabilitation works, the performance will gain a recovery to an acceptable level f_r. Then the resilience could be explained by the ratio of the residual performance area (shaded by green in Figure 25) over the total performance area (green shade plus the red shade area):

$$\mathrm{Re} = \frac{A_r}{A_r + A_{loss}} \tag{13}$$

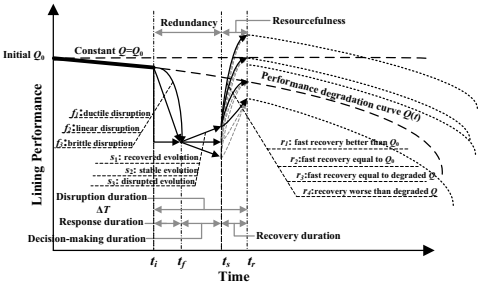

Figure 26. Different type performance transition curves in the resilient analysis

The current practice for the tunnel repair works after a disruption happens seldom has cost-benefit assessment for repair efficiency. It usually results in a high cost but low effect on the performance recovery. However, by applying the resilience analysis, the efficiency could be mathematically calculated by the area ratio using Eq. 13 and graphically reflected by Figure 26, in which different types of performance transition curves are compared. Different residual performance f_i and recovery performance f_r could clearly cause the difference of the final resilience. Then the most resilient strategy could be decided for the tunnel repair or designs. Even given the same f_i, f_d and f_r, the resilience of tunnels with different transition curves could be of great difference between each other and affect the decision making process for tunnel repair works.

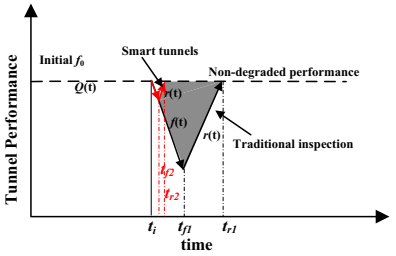

Figure 27. Effect of the rapidity on the tunnel resilience

Note that the resilience concept described by Figure 25 strongly depends on the time t. A quick reaction on the disruption caused by the threats to the tunnels could gain the most recovery at the lowest cost, which is visually demonstrated by Figure 27. If the tunnels has been instrumented by the smart measurement or inspection techniques, the disruption of the performance could be captured once it occurs. Then the recovery cost could be significantly lower than those for a traditional instrumented tunnels. If the performance degradation is ignored at this moment, the loss of the total performance could reduce by the square relationship of the disruption. On the other hand, the resilient ability for tunnels could be increased, which means that the threats to the tunnels are insignificant.

A real case study has been carried out recently by applying the resilience concept

into the interpretation of the effect of the rapidity on the tunnel performance recovery. Figure 28 has illustrated the integrated convergence performance transition once an extreme large surcharge has been loaded on the ground above the tunnel. Almost six years has been passed since the occurrence of the disruption until the complete of the recovery. The slowness of the reaction has resulted in a small resilience index Re (see Eq. 13) at 0.34. It means that 66% of the total performance has been lost because of the extreme surcharge and also because of the slow reaction.

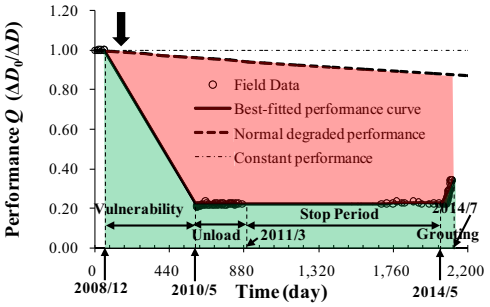

Figure 28. Measured performance transition for tunnel convergence in a case of Shanghai

If there were a similar case to the real one but only except that the tunnel has been instrumented by real-time wireless sensor network for measurement and inspection. If the smart technique, i.e., WSN, can capture the disruption within 80 days after the surcharge loading on the ground, the 11% loss of the performance could be fully recovered by the grouting, which results in a high resilience index Re at 0.94. It would be significantly larger than the previous one at 0.34 for the real case. This comparison is visually explained by Figure 29. Hence, 60% of the tunnel resilient ability has been increased if the rapidity is appreciated using the real-time measurement. With the help of resilience analysis, the effect of residual performance subjected to the extreme threats and the recovery rapidity on the system lifetime performance could be explicitly explained by Eq. 13 or Figure 25.

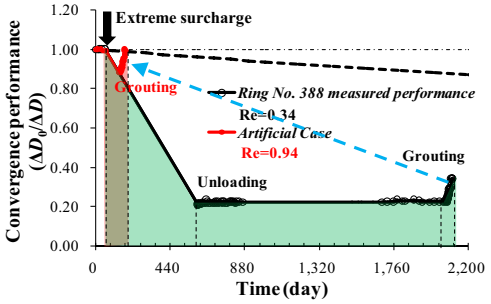

Figure 29. Comparison of the resilience between real case and artificial case

8. Projects Application

The milestone of applying the quantitative risk management (QRM) to tunnel project in China should be the application into the Shanghai Yangtze River Tunnel in 2002. The Shanghai Yangtze River Tunnel has a length of 8.9km and an outer-diameter of 15m, which is the biggest tunnel in the world at that time. It was designed to be constructed by a slurry-balance shield machine. The tunnel locates at the Yangtze estuary in Shanghai. The geological condition is significantly challenging.

In total, twelve sessions of risk of the project from design phase to the operation phase has been quantitatively assessed, including river evolution, ecological environment, geological environment, the bridge wind resistance, operation management, ship collision, structure stability and water resistant, shield machine design analysis, engineering, tunnel ventilation, tunnel fire hazard, terrorist attack, traffic volume forecast, anti-seismic, durability of structure, bridge foundation. The risk concept has been successfully introduced into the construction and operation of the tunnel for the lifetime risk management.

Recently, the QRM also has been successfully applied into the Hong Kong-Zhuhai-Macao bridge, which is inter-regional huge infrastructure project in southeast of China. The project consists of the construction of cable-stayed bridge and the immersed tube tunnel, in which the tunnel is the most challenging part. Each tube of the tunnel has a length of 180m, a height of 11.4m and a width of 37.95m, which is the biggest tube in the

world at present. The tunnel has a total length of 6.7km. The quantitative risk assessment has been applied both for the bridge and tunnel part. In addition, detailed numerical studies and centrifuge model test are still ongoing to be carried out for the validation of the assessed risk.

Besides, to date, the QRM has been applied into eight under-water tunnel projects in China at the plan and design stage. The risks of the urban rail transit system during the construction stage has been quantitatively assessed and managed by the QRM in China, such as the metro in Beijing, Shanghai, Suzhou, Wuhan and Wuxi. Nowadays, as the Code has been put into effect, the QRM is compulsory for a urban rail transit system in China during the plan, design and construction stages.

9. Conclusion

In China, the risk management associated with tunnel projects was formally put into action ten years ago with the fast development of tunneling. Some practical experiences and research analysis on risk management are shared in this paper, including the hazard identification, quantitative risk assessment, dynamic risk management and risk control in visualization. The on-going research on tunnel resilience for the high-impact low-chance risk is also presented. Some of the concluding remarks could be summarized as below:

1) The quantitative risk assessment applied in China has included fuzzy fault tree analysis for the hazard identification, conditional Markov chain for the probability of soil spatial distribution, quantitative vulnerability analysis for the consequence evaluation. The risk acceptance criteria has been set up based on field case of structural failures in China. All the above techniques has been validated by its practical application into real cases.

2) As risk would vary with the time, the dynamic feature of risk during the lifetime of tunnel structures should be greatly appreciated for management. It is crucial for safety control of a tunnel even when the risk is analyzed in a qualitative manner. The visualization of the risk via the recent developed LEDs and MEMs coupled with WSN techniques is of great efficiency to inform the workers on site in real-time.

3) The tunnel resilience subjected to the disruption caused by the high-impact low-chance risk could be quantitatively evaluated by using the proposed resilience model. With smart monitoring and inspection techniques, the performance robustness subjected to the hazard and the rapidity of performance recovery could be enhanced with a minimized time and monetary cost. Thus, the risk after disaster could be controlled effectively.

References

Ang, A. H.-S., and Tang, W. H. (1975). *Probability Concepts in Engineering Planning and Design*, Wiley.

Bian, Y. H., and Huang, H. W. "Fuzzy fault tree analysis of failure probability of smw retaining structures in deep excavation." *Proc., GeoShanghai International Conference 2006: Underground Construction and Ground Movement (GSP 155)*, ASCE.

Burland, J. B., and Wroth, C. "Settlement of buildings and associated damage." *Proc., Proc., Conference on Settlement of Structures*.

Casagrande, A. (1965). "Role of the" calculated risk" in earthwork and foundation engineering-The second Terzaghi Lecture." *Journal of the Soil Mechanics and Foundations Division*, 91(4), 1-40.

CEDD-GEO (2005). "Guidelines for Risk Management of Geotechnical Engineering in Hongkong." Civil Engineering and Development Department Geotechnical Engineering Office, Hongkong.

DB11/1067 (2013). "Code for safety risk assessment of urban rail transit engineering design (DB11/1067-2013)." Beijing Urban Plan Committee, Beijing.

GB50652-2011 (2012). "Code for risk management of underground works in urban transit (GB50652-2011)." Ministry of Housing and Urban-Rural Development (MOHURD), Beijing.

Hu, Q., and Huang, H. "Risk analysis of soil transition in tunnel works." *Proc., ITA-AITES World Tunnel Congress 2007*

Huang, H., and Chen, L. "Risk analysis of building structure due to shield tunneling in urban area." *Proc., GeoShanghai International Conference 2006: Underground Construction and Ground Movement (GSP 155)*, ASCE, 150.

Huang, H. W. (2006). "State-of-the-Art of the Research on Risk Management in Construction of Tunnel and Underground Works." *Chinese Journal of Underground Space and Engineering*, 2(1), 13-20 (in Chinese).

Huang, H. W., Xu, R., and Zhang, W. (2013). "Comparative Performance Test of an Inclinometer Wireless Smart Sensor Prototype for Subway Tunnel." *International Journal of Architecture, Engineering and Construction*, 2(1), 25-34.

Huang, X., and Huang, H. W. "Vulnerability Evaluation of Shield Tunnel Under the Effect of Above Excavation." *Proc., Tunnelling and Underground Space Construction for Sustainable Development*, CIR Publishing.

ILO (2003). "Annual report for record of deadly accident for occupational safety in the world." International Labor Organization, Geneva.

ITA (2002). "Guidelines for tunneling risk management." International Tunnel Association Working Group No. 2 217-237.

ITA (2014). "Guidelines on Monit oring Frequencies in Urban Tunnelling." International Tunnelling and Underground Space Association, Longrine, France.

Lacasse, S. (2015). "Hazard, Risk and Reliability in Geotechnical Practice: 55th Rankine Lecture." British Geotechnical Association, London.

Latham, M. (1994). "Constructing the Team: Final Report of the Government/ Industry Review of Procurement & Constractual Arrangements in the UK Construction Industry." HSMO, London.

Li, Z., Huang, H., Nadim, F., and Xue, Y. (2010). "Quantitative risk assessment of cut-slope projects under construction." *Journal of Geotechnical and Geoenvironmental Engineering*, 136(12), 1644-1654.

Li, Z., Huang, H., and Xue, Y. (2014). "Cut-slope versus shallow tunnel: Risk-based decision making framework for alternative selection." *Engineering Geology*, 176, 11-23.

Li, Z., Nadim, F., Huang, H., Uzielli, M., and Lacasse, S. (2010). "Quantitative vulnerability estimation for scenario-based landslide hazards." *Landslides*, 7(2), 125-134.

Liu, Z., Huang, H., and Xue, Y. (2009). "The application of quantitative risk assessment in talus slope risk analysis." *Georisk*, 3(3), 155-163.

MOHURD (2007). "Guideline of risk management for construction of subway and underground works." Ministry of Housing and Urban-Rural Development (MOHURD), Beijing.

MRPRC (2007). "Regulation of risk assessment and management for railway tunnel." (Ex) Ministry of Railway of People's Republic of China, Beijing.

MTPRC (2010). "Guideline for safety risk assessment of design for road bridge and tunnel." Ministry of Transportation of People's Republic of China, Beijing.

MTPRC (2011). "Guideline for safety risk assessment of construction for road bridge and tunnel." Ministry of Transportation of People's Republic of China, Beijing.

Nadim, F., and Liu, Z. "Quantitative risk assessment for earthquake-triggered landslides using Bayesian network." *Proc., Proceedings of the 18th international conference on soil mechanics and geotechnical engineering, Paris*.

Shen, X. D., Huang, H. W., Zhang, D. M., and Zhang, J. "Vulnerability Assessment of Shield Tunnel under Surcharge in Soft Soils." *Proc., 27th KKHTCNN Symposium on Civil Engineering*.

Tang, W. H. "Principles of probabilistic characterization of soil properties." *Proc., Probabilistic characterization of soil properties: bridge between theory and practice*.

Uzielli, M., Nadim, F., Lacasse, S., and Kaynia, A. M. (2008). "A conceptual framework for quantitative estimation of physical vulnerability to landslides." *Engineering Geology*, 102(3), 251-256.

Whitman, R. V. (1984). "Evaluating calculated risk in geotechnical engineering." *Journal of Geotechnical Engineering*, 110(2), 143-188.

Whitman, R. V. (2000). "Organizing and evaluating uncertainty in geotechnical engineering." *J. Geotech. Geoenviron. Eng.*, 126(7), 583-593.

Yan, Y., Huang, H., and Hu, Q. "Risk analysis for cutterhead failure of composite EPB shield based on fuzzy fault tree." *Proc., The 6th International Aspects of Underground Construction in Soft Groud. London: Taylor & Francis Group*.

Zhang, L. L., Tang, W. H., and Zhang, L. M. (2009). "Bayesian Model Calibration Using Geotechnical Centrifuge Tests." *J. Geotech. Geoenviron. Eng.*, 135(2), 291-299.